Environ Health Eng Manag 2027;14:1859
http://ehemj.com

doi:10.34172/EHEM.1859

Environmental Health Engineering and Management Journal

Original Article

Environmental Health Engineering and Management

Open Access Publish Free

Ecological and Human Health Risks of Heavy Metal Contamination in Soils From Artisanal Gold Mining in Sidama, Ethiopia

Samuel Bekele[1*], Teferi Shanka[2], Muluken Andemo[1], Tesfahun Tesema[1]

[1]Department of Environmental Science, Hawassa University, Ethiopia
[2]Department of Soil Resources and Watershed Management, Hawassa University, Ethiopia

Abstract

Introduction: Mining poses ecological and human health risks through heavy metal contamination. This study assessed contamination, ecological risk, potential sources, and human-health implications in soils surrounding the Osole gold mining area, Sidama, Ethiopia.

Methods: Eleven metals (As, Cd, Hg, Pb, Ni, Cr, Fe, Co, Zn, Mn, and Cu) were quantified using inductively coupled plasma optical emission spectrometry (ICP–OES). Contamination was evaluated using CF, Cdeg, mCdeg, and PLI, and ecological risk using ER and ERI. Pearson's correlation, principal component analysis (PCA), and hierarchical cluster analysis (HCA) assessed metal associations and potential sources. Human-health risks were evaluated using the USEPA framework.

Results: Metal concentrations followed the order Fe>Mn>Zn>Cr>Cu>Ni>Pb>Co>Cd>Hg>As. Cd and Hg exceeded agricultural soil guideline values at all sites and were the principal contributors to contamination and ecological risk. Contamination indices indicated high to very high contamination, while ER and ERI indicated very high ecological risk. Multivariate analyses suggested geogenic and anthropogenic inputs associated with mining activities. Individual non-carcinogenic risks were below the acceptable threshold (HQ<1), but cumulative risk exceeded the acceptable level for children. Ni and Cr were the principal contributors to carcinogenic risk, with potential lifetime cancer risks for children at all sites and adults at SG1 and SG3.

Conclusion: Cd and Hg were priority contaminants, and children were the most vulnerable receptor. The findings support improved mine-waste management and protection of mining-affected agricultural soils.

Keywords: Ecological risk assessment, Gold mining, Human health risk assessment, Heavy metals, Soil contamination

Citation: Bekele S, Shanka T, Andemo M, Tesema T. Ecological and human health risks of heavy metal contamination in soils from artisanal gold mining in sidama, ethiopia. Environ Health Eng Manag 2027;14:1859. doi:10.34172/EHEM.1859

Article History:
Received: February 3, 2026
Revised: August 18, 2026
Accepted: August 22, 2026
ePublished: November 3, 2026

***Correspondence to:**
Samuel Bekele,
Email: beksam10@gmail.com

Introduction

Heavy metal contamination of soils represents a major environmental challenge worldwide because of the persistence, toxicity, and long-term ecological and human-health implications of these contaminants. Mining activities are among the principal anthropogenic sources of heavy metal accumulation, as excavation, mineral processing, and waste disposal can enhance the mobilization of naturally occurring elements into surrounding terrestrial environments (1,2). Once released, heavy metals can persist in soils for decades, accumulate in agricultural systems, alter soil functions, and enter food chains through plant uptake, dust inhalation, dermal contact, and incidental soil ingestion (3-5). Understanding heavy metal distribution, environmental behavior, and associated risks is therefore essential for sustainable land management and the protection of ecosystem and human health.

Artisanal and small-scale gold mining (ASGM) is one of the fastest-growing mining sectors worldwide, supporting the livelihoods of millions of people while generating significant environmental challenges due to inefficient extraction techniques, inadequate waste management, and limited regulatory control (6). Mercury used during gold amalgamation, together with excavation of mineralized rocks and disposal of mine wastes, can enhance the release of Hg and other heavy metals, including As, Cd, Pb, Cr, Ni, Co, Cu, Zn, Fe, and Mn, into surrounding soils (4,7,8). The distribution and mobility of these elements are influenced by interactions among mining activities, geological characteristics, weathering processes, and soil properties. Consequently, ASGM-affected environments commonly contain complex mixtures of contaminants, requiring multi-element evaluation rather than assessment of individual pollutants alone.

© 2027 The Author(s). Published by Kerman University of Medical Sciences. This is an open-access article distributed under the terms of the Creative Commons Attribution License (http://creativecommons.org/licenses/by/4.0), which permits unrestricted use, distribution, and reproduction in any medium, provided the original work is properly cited.

Previous studies have reported elevated heavy metal concentrations in ASGM-affected soils across Africa and other developing regions. However, many investigations have focused primarily on contamination levels or individual pollution indices, while fewer have integrated multi-element characterization, ecological risk assessment, multivariate statistical analysis, and quantitative human-health risk evaluation within a single framework. Consequently, the factors influencing heavy metal distribution, element associations, ecological significance, and cumulative exposure risks remain insufficiently understood, particularly in rapidly expanding ASGM regions where environmental monitoring capacity is limited. Addressing these knowledge gaps is important for developing effective risk-based management and pollution-control strategies.

Ethiopia possesses considerable gold resources and has experienced rapid expansion of ASGM during recent decades. Although the sector contributes to rural livelihoods and local economic development, increasing mining activities have raised concerns regarding environmental degradation because extraction commonly occurs near agricultural land with limited environmental oversight. Previous studies have reported elevated levels of Hg and other Heavy metals in Ethiopian mining environments (3,9-12). Nevertheless, these studies have largely emphasized contaminant occurrence or pollution status, with limited integration of element relationships, ecological risks, and human-health implications within a unified assessment framework.

The Osole gold-mining area in Chabe Gambeltu Woreda, Sidama Regional State, represents an emerging ASGM landscape where mining activities occur in proximity to cultivated land. Despite continued mining expansion, comprehensive information on multi-element contamination patterns, ecological risks, element associations, and potential human-health implications in soils from this area has not been reported. This lack of baseline information limits understanding of the extent and significance of mining-related contamination and constrains the development of effective monitoring and pollution-management strategies.

Accordingly, this study presents an integrated assessment of heavy metal contamination, ecological risks, element associations, and human-health implications in soils from the Osole gold-mining area. Eleven Heavy metals (As, Cd, Hg, Pb, Ni, Cr, Fe, Co, Cu, Zn, and Mn) were quantified using inductively coupled plasma optical emission spectrometry (ICP–OES). Contamination characteristics and ecological risks were evaluated using established contamination indices, while element relationships and potential source-related patterns were investigated using Pearson's correlation analysis, principal component analysis (PCA), and hierarchical cluster analysis (HCA). Human-health risks for adults and children were assessed using the USEPA risk assessment framework. By integrating these complementary approaches, this study establishes a comprehensive baseline for an understudied Ethiopian ASGM landscape, identifies priority contaminants and vulnerable receptors, and provides scientific evidence to support risk-based environmental monitoring, improved mine-waste management, and sustainable management of mining-affected agricultural soils.

Materials and Methods

Description of the study area

The study was conducted in Chabe Gambeltu Woreda, Osole Kebele (6°21′20″–6°24′19″ N; 38°47′3″–38°50′25″E), Sidama Regional State, Ethiopia (Figure 1). The site lies 161 km from Hawassa, the regional capital, and 441 km south of Addis Ababa, the national capital. Elevation ranges between 1300 and 2400 m above sea level. The climate is equatorial monsoon-type, with annual rainfall of 700–1400 mm and mean temperatures ranging from 10 to 30°C. The

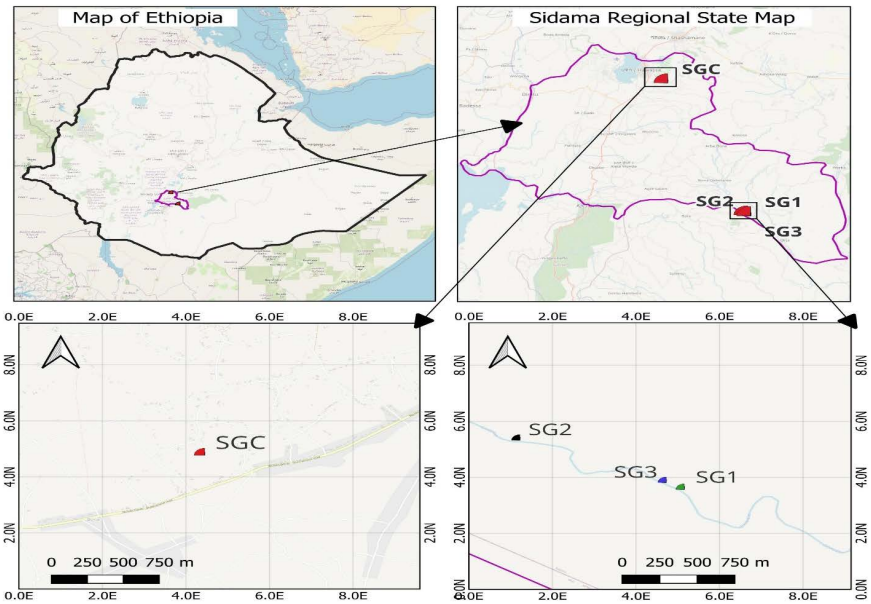


Figure 1. Location map of the Osole gold mining area showing the distribution of soil sampling sites and the comparative reference site (SGC)

terrain is rugged and dissected, dominated by the Genale River and its tributaries (Ganbeltu River), which provide perennial flow. Vegetation consists of scrubs, bushland, eucalyptus stands, and woodlands, particularly at high altitudes and valley slopes. Farmland is mainly located in elevated and gently sloping areas, where coffee, enset (*Ensete ventricosum* (Welw.) Cheesman), a perennial crop widely cultivated for food in Ethiopia, maize, and other crops are cultivated. Soils are deeply weathered and variable across altitudinal zones.

Economically, coffee is the major cash crop, supplemented by livestock rearing. Artisanal gold mining has long been practiced in the area, while mechanized mining has emerged only within the past six years. Settlements are unevenly distributed: permanent villages are established in fertile highlands and along riverbanks, whereas seasonal settlements are common near the Ganbeltu River. Many households depend on artisanal mining and small-scale livestock farming as their primary livelihoods. Geologically, the area is rich in primary and secondary gold mineralization. The Genale and Galana rivers cross mineralized and altered rock zones, creating extensive placer gold deposits along their banks. Active and abandoned mining sites are widespread, with licenses typically granted to local associations that collaborate with private investors under a 70:30 profit-sharing arrangement. The commercial mining areas cover approximately 18,785.6 m^2 (1.88 ha). Mercury and cyanide are commonly used in gold processing, and current production exceeds 170 kg per year.

Sampling site selection and sample collection

Soil samples were collected from areas surrounding the Osole artisanal and small-scale gold mining (ASGM) sites in Chabe Woreda, Sidama Regional State, Ethiopia, together with a comparative reference site located in Wondo Genet. Three mining-influenced sites were selected along the downstream gradient of mining activities. Site SG1 was located near the primary mining discharge zone, representing the area of greatest direct influence from mining operations. SG2 was located approximately 1.0 km downstream of SG1, representing an intermediate influence zone, while SG3 was positioned an additional 500 m downstream of SG2 to represent the lower influence zone. Site SGC, located approximately 74 km northwest of the mining area in Wondo Genet, was selected as a comparative reference site because it is outside the direct influence of mining, industrial activities, and major urban disturbances while sharing similar regional environmental conditions (Figure 1).

At each site, 10 composite topsoil samples (0–15 cm depth) were randomly collected using a soil coring procedure following the USEPA soil sampling guidelines (13). Sample collection, preparation, and analysis followed established soil analytical procedures (14,15). Samples were placed in pre-cleaned polyethylene bags, labeled, and transported in ice-filled containers to the Horticop Laboratory, Bishoftu, Ethiopia.

Special precautions were applied for mercury analysis because of its volatility. Samples were stored in airtight containers, maintained under cooled conditions during transport, and analyzed promptly after laboratory arrival to minimize potential Hg losses. All samples were collected during a single dry-season field campaign in February 2025.

Sample preparation and analysis for heavy metals

In the laboratory, soil samples were air-dried for three days, homogenized, and passed through a 2 mm polyethylene sieve. A 0.25 g aliquot of each dried sample was transferred into closed Teflon digestion vessels, followed by the addition of 5 mL ultrapure nitric acid (HNO_3). Microwave-assisted digestion was performed using an Ultraclave system (Milestone, Italy) at 260°C for 1.5 h following the procedure described by Yüksel et al. (16). The digested solutions were diluted with ultrapure Milli-Q water and analyzed for total concentrations of As, Cd, Hg, Pb, Ni, Cr, Fe, Co, Cu, Zn, and Mn using inductively coupled plasma optical emission spectrometry (ICP-OES; PerkinElmer Optima 8000).

Quality assurance and quality control procedures, including analytical blanks, calibration standards, detection limits, and certified reference material analysis, are described in Section 2.8. The accuracy of elemental determination was evaluated using the certified reference material SRM 2711a Montana II Soil, with recoveries ranging from 95–105%.

Total Hg concentrations were determined using ICP-OES to evaluate overall Hg contamination associated with mining activities. Although mercury speciation methods such as cold vapor atomic absorption spectroscopy (CV-AAS) and methylmercury analysis provide information on Hg transformation and bioavailability, this study focused on total Hg concentrations because the primary objective was to characterize overall contamination levels and associated ecological and human-health risks. The application of certified reference material validation and controlled sample handling ensured reliable total Hg quantification.

Because Hg can be susceptible to volatilization during sample handling and drying, the three-day air-drying step represents a potential source of uncertainty in the measured total Hg concentrations. Although samples were collected, transported, and stored under conditions intended to minimize Hg loss, drying at room temperature may have resulted in some volatilization of Hg prior to analysis. Therefore, the reported Hg concentrations should be interpreted as measured total Hg concentrations under the applied sample-preparation procedure and may represent conservative estimates of the original field Hg burden.

Physicochemical properties of soils

Soil organic carbon (OC) content was determined using the loss-on-ignition (LOI) method, in which oven-dried samples were heated at 550°C for 4 hours (17). Cation exchange capacity (CEC) was measured with sodium acetate and ammonium acetate solutions following the

standard procedures described by Loring and Rantala (18). Soil pH was measured using a calibrated digital pH meter (19). Soil texture, including sand (0.05–2 mm), silt (0.002–0.05 mm), and clay (< 0.002 mm) fractions, was determined using the hydrometer method (20) (Table S1).

Statistical analysis

All statistical analyses were performed using IBM SPSS Statistics version 30.0 and RStudio. Descriptive statistics were calculated for all measured Heavy metals. One-way analysis of variance (ANOVA) was used to evaluate differences in heavy metal concentrations among the four sampling sites (SG1, SG2, SG3, and SGC). The assumptions of normality and homogeneity of variances were assessed using the Shapiro–Wilk and Levene's tests, respectively. When significant differences were detected ($\alpha = 0.05$), Tukey's honestly significant difference (HSD) test was applied for post-hoc comparisons, and effect sizes were estimated using eta-squared (η^2).

Pearson's correlation analysis was performed to evaluate relationships among heavy metals using two-tailed tests with significance levels of $P < 0.05$ and $P < 0.01$. Multivariate statistical analyses, including principal component analysis (PCA) and hierarchical cluster analysis (HCA), were conducted using Z-score standardized heavy metal data. Before PCA, the suitability of the dataset was evaluated using the Kaiser–Meyer–Olkin (KMO) measure of sampling adequacy and Bartlett's test of sphericity. Principal component analysis (PCA) was performed using the correlation matrix with Varimax rotation and Kaiser normalization to identify associations among heavy metals and determine the major factors influencing their distribution. Hierarchical cluster analysis (HCA) was conducted on standardized elemental concentrations using Ward's minimum variance method (Ward.D2) with Euclidean distance to classify heavy metals based on their geochemical similarities and identify distinct elemental associations in gold mining-impacted soils.

Ecological risk assessment of heavy metals in soils

The potential ecological risks of heavy metals in soils around the Osole gold mining areas in Chabe Woreda were evaluated using several indices, including the contamination factor (CF), degree of contamination (Cdeg), modified degree of contamination (mCdeg), single-element potential risk factor (ER), potential ecological risk index (ERI), and pollution load index (PLI), as outlined below:

Contamination factor (CF)

The contamination factor (CF) is used to quantify the level of heavy metal contamination in soils (21). Although originally developed for lake sediments, this approach has been used for heavy metal soil assessments (22,23). CF is calculated as the ratio of the measured concentration of a heavy metal in the soil to its corresponding pre-industrial or background reference value, as expressed in Equation (1):

$$CF = \frac{C}{Cr} \quad (1)$$

Where C is the concentration of the metal in soil (mg/kg), and C_r is the pre-industrial reference value/baseline level or national criteria for heavy metals in soils.

As there are no pre-industrial heavy metal concentration data for soils in the study area, nor established national soil quality standards in Ethiopia, average global background values for uncontaminated agricultural soils were used as reference levels (24,25). These global background values provide a standardized benchmark for environmental assessment and allow meaningful comparisons across regions and studies. They are also considered more appropriate for assessing environmental risk in agricultural soils than crustal abundance values, which are typically used in geological studies.

The reference values for heavy metals in this study were: As (5.0 mg/kg), Cd (0.15 mg/kg), Hg (0.1 mg/kg), Pb (17 mg/kg), Ni (40 mg/kg), Cr (70 mg/kg), Fe (35,000 mg/kg), Co (10 mg/kg), Cu (25 mg/kg), Zn (70 mg/kg), and Mn (600 mg/kg).

It should be noted that contamination factor (CF), ecological risk factor (ER), and ecological risk index (ERI) calculations depend on the choice of reference values. The potential variability of these indices under alternative baselines is evaluated in the results section, where sensitivity considerations for metals with low (Cd, Hg) and high (Fe, Cr) natural variability are discussed.

According to the study by Håkanson (21), the CF is categorized as:

- CF < 1: Low contamination
- 1 < CF < 3: Moderate contamination
- 3 < CF < 6: Considerable contamination
- CF > 6: Very high contamination.

Degree of contamination (Cdeg)

The degree of contamination (Cdeg) offers an overall assessment of soil contamination by integrating the contamination factors (CF) of individual heavy metals (26). It is determined as the sum of all contamination factors, as expressed in Equation 2:

$$\boldsymbol{Cdeg} = \sum_{i=1}^{n} CF \quad (2)$$

Where n is the number of analyzed elements, $i = i^{th}$ element, and CF is the contamination factor.

According to the study by Håkanson (21), the degree of contamination is rated as:

- Cdeg < 6: Low degree of contamination
- 6 < Cdeg < 12: Moderate degree of contamination
- 12 < Cdeg < 24: Considerable degree of contamination
- Cdeg > 24: Very high degree of contamination

Modified degree of contamination (mCdeg)

The modified degree of contamination (mCdeg) was developed to evaluate the overall level of contamination at a given site (26). It is calculated as the total sum of contamination factors (CF) divided by the number of heavy metals analyzed, as shown in Equation 3:

$$mCdeg = \frac{\sum_{i=1}^{i=n} CF}{n} \quad (3)$$

Where n represents the number of analyzed elements, i denotes the i^{th} element, and CF is the contamination factor. The modified degree of contamination (mCdeg) is classified according to the study by Håkanson (21) as follows:

- mCdeg < 1.5: Very low contamination
- 1.5 < mCdeg < 2: Low contamination
- 2 < mCdeg < 4: Moderate contamination
- 4 < mCdeg < 8: High contamination
- 8 < mCdeg < 16: Very high contamination
- 16 < mCdeg < 32: Extremely high contamination
- mCdeg > 32: Ultra-high contamination

Potential ecological risk factor (ER)

The ecological risk factor (ER), proposed by Håkanson (21), combines an element's contamination factor with its toxic response factor to quantify the potential ecological risk it poses. It is calculated using Equation (4):

$$Er = TrCF \quad (4)$$

Where Tr is the toxic-response factor for a given element, with values of As = 10, Cd = 30, Hg = 40, Pb = 5, Ni = 5, Cr = 2, Co = 5, Cu = 5, Zn = 1, and Mn = 1, as proposed by Håkanson (21). CF is the contamination factor of each metal. According to the study by Håkanson (21), the potential ecological risk was classified based on ER values as:

- ER < 40: Low potential ecological risk
- 40 < ER < 80: Moderate potential ecological risk
- 80 < ER < 160: Considerable potential ecological risk
- 160 < ER < 320: High potential ecological risk
- ER > 320: Very high potential ecological risks

Potential ecological risk index (ERI)

The potential ecological risk index (ERI) is a widely applied approach for assessing heavy metal pollution in soils. This index incorporates both heavy metal concentrations and their toxicological characteristics to evaluate the degree of contamination and associated ecological risks (26). It is expressed as the sum of the individual ecological risk factors (ER) for all analyzed metals (21), as shown in Equation 5:

$$ERI = \sum_{i=1}^{n} Er \quad (5)$$

According to the study by Håkanson (21), the potential ecological index was classified as: ERI < 100, low risk; 100 < ERI < 150, moderate risk; 150 < ERI < 200, considerable risk; 200 < ERI < 300, high risk; and ERI > 300, very high risk.

Pollution load index (PLI)

The pollution load index (PLI), introduced by Tomlinson et al. (27), offers a straightforward comparative measure of the overall level of heavy metal contamination. It is used to evaluate the degree of pollution at each sampling site based on combined contamination factors, and is calculated as shown in Equation 6:

$$PLI = \left(CF1 \times CF2 \times CF3X \ldots.. \times CFn\right)^{1/n} \quad (6)$$

Where CF is the contamination factor; n is the number of metals analyzed, and CFn is the contamination factor for n*th* element, as described above. According to the study by Tomlinson et al. (27), a PLI value < 1 indicates no pollution, whereas a value > 1 signifies the presence of metal pollution.

Human health risk assessment

Human health risk assessment was conducted to evaluate potential risks from soil contamination through three primary exposure pathways: direct soil ingestion, inhalation of dust particles, and dermal absorption following the guidelines of the U.S. Environmental Protection Agency (28). The assessment estimated non-carcinogenic risks using the hazard quotient (HQ) and hazard index (HI) and evaluated cancer risk (CR) and total cancer risk (TCR) for carcinogenic metals. Separate assessments were conducted for children and adults based on age-specific exposure factors (Table S2). The total hazard quotient (THQ) was estimated as the cumulative non-carcinogenic risk for a given metal across all exposure pathways. The hazard index (HI) was calculated by summing the HQ values across all metals.

$$ADD_ingestion = \frac{C_soil \times IngR \times EF \times ED \times CF}{BW \times AT} \quad (7)$$

$$ADD_inhalation = \frac{C_soil \times InhR \times EF \times ED}{BW \times AT \times PEF} \quad (8)$$

$$ADD_dermal = \frac{C_soil \times AF \times SA \times ABS \times EF \times ED \times CF}{BW \times AT} \quad (9)$$

Where C_{soil} is the heavy metal concentration in soil (mg/kg), $IngR$ is the soil ingestion rate (mg/day), $InhR$ is the inhalation rate (m^3/day), EF is the exposure frequency (day/year), ED is the exposure duration (year), CF is the conversion factor (kg/mg), BW is average body weight (kg), AT is averaging time (day), AF is skin adherence factor (mg/cm^2/day), SA is exposed skin area (cm^2), ABS is dermal absorption factor (unitless), and PEF is particle emission factor (m^3/kg).

The values for these parameters were given in a separate table (Table S2). Due to limited local exposure data, default USEPA values and probability distributions were used for the risk calculations.

Non-carcinogenic risk

The hazard quotient (HQ) and hazard index (HI) indices were used to estimate non-carcinogenic human health risks. The HQ for an individual metal was calculated as the ratio of ADD to the reference dose (RfD), as in Equation 10.

$$HQ = \frac{ADD}{RfD} \quad (10)$$

$$THQ = \sum HQ_ing + HQ_inh + HQ_derm \quad (11)$$

Where **RfD** is the reference dose (mg/kg/day).

Hazard index (HI) was estimated as:

$$HI = \sum HQi \quad (12)$$

$$THI = \sum THQ \quad (13)$$

If THQ or THI ≤ 1, there is no adverse human health effect, and if THQ or THI ≥ 1, there is a potential non-carcinogenic risk (29).

Carcinogenic risks

Based on the International Agency for Research on Cancer (30), heavy metals such as As, Cd, Pb, Ni, and Cr are considered to have a carcinogenic effect. The incremental lifetime cancer risk (ILCR) for each carcinogenic metal was estimated using Equation 14 as:

$$CRi = AddixSF \quad (14)$$

Where *SF* is the cancer slope factor (kg/day/mg).

The cumulative carcinogenic risk for a given metal across all exposure pathways was calculated as:

$$CR = \sum CR_ing + CR_inh + CR_derm \quad (15)$$

According to the USEPA (31) guideline, if CR is greater than or equal to 1 x 10^{-4}, there is a carcinogenic risk. The values for SF and RfD are listed in Table S3.

Quality assurance/quality control (QA/QC)

To ensure the reliability and accuracy of elemental determination, comprehensive QA/QC procedures were implemented throughout soil analysis. Method blanks, laboratory blanks, and duplicate samples were analyzed with each analytical batch to evaluate potential contamination and analytical precision. Certified reference material (CRM; NIST SRM 2711a Montana Soil) was digested and analyzed under the same conditions as samples to assess analytical accuracy, with elemental recoveries ranging from 95–105%.

ICP-OES calibration was performed using multi-element standard solutions prepared at five concentration levels, producing linear calibration curves with regression coefficients (R^2) ≥ 0.999. Limits of detection (LOD) and limits of quantification (LOQ) were calculated as three and 10 times the standard deviation of method blanks, respectively. The calculated LOD and LOQ values for each element are presented in Table S4, and measured concentrations were above the corresponding LOQs.

Analytical accuracy was further verified through matrix spike recovery tests, in which representative soil samples were fortified with known analyte concentrations. Recovery values ranged from 92–106%, confirming the reliability of the digestion and analytical procedures. Analytical precision was evaluated through replicate analyses, with relative standard deviations (RSDs) generally below 5% for most trace elements. Slightly higher variability observed for Fe and Mn was attributed to natural soil heterogeneity and their relatively high abundance in soil matrices.

Because mercury was identified as a priority contaminant in the study area, additional validation was considered essential. The LOD and LOQ for Hg were 0.05 and 0.15 mg kg^{-1}, respectively (Table S3). Recovery of Hg from the certified reference material (NIST SRM 2711a) was 101%, and matrix spike recoveries were within the acceptable range (92–106%), confirming the reliability of total Hg determination by ICP-OES. Overall, the QA/QC results demonstrated that the analytical method was suitable for accurate determination of heavy metal concentrations in mining-impacted soils.

Results

Concentration of heavy metals in soils

The mean concentrations of heavy metals in soils from the artisanal and small-scale gold mining (ASGM)-impacted sites (SG1, SG2, and SG3) and the comparative reference site (SGC) are presented in Table 1. The overall abundance sequence was Fe > Mn > Zn > Cr > Cu > Ni > Pb > Co > Cd > Hg > As, indicating the predominance of major lithogenic elements and the variable distribution of trace elements within the studied soils (32).

Mining-impacted soils generally exhibited higher concentrations of Cd, Hg, Pb, Cr, Cu, Fe, Co, and Mn compared with the reference site, demonstrating spatial variability associated with mining disturbance, geological characteristics, and site-specific geochemical conditions. The highest concentrations of Cd (6.41 mg/kg), Hg (6.23 mg/kg), Cu (44.73 mg/kg), and Co (26.51 mg/kg) were recorded at SG1, suggesting greater enrichment at the most mining-influenced site. In contrast, Zn concentrations were higher at the reference site than at SG2 and SG3, indicating that Zn distribution may be controlled by factors beyond mining inputs, including parent material composition, soil properties, and element-specific mobility. One-way ANOVA revealed significant differences among sampling sites for most investigated elements ($P < 0.05$), confirming spatial heterogeneity in heavy metal distribution. Comparison with Dutch Target Values showed that Cd and Hg concentrations exceeded the corresponding screening values at all mining-impacted sites, while Cu exceeded the guideline value only at SG1.

Mean As concentrations ranged from 0.96 to 1.37 mg/kg, with the highest value recorded at SG1 and the lowest value at the comparative reference site (SGC) (Table 1). Mining-impacted soils exhibited only slightly higher As concentrations than the reference soil, and all measured values remained well below the Dutch Target Value for soil quality (29 mg/kg), indicating limited As enrichment in the studied mining area. Similarly, mean Cd concentrations in mining-impacted soils ranged from 3.46 to 6.41 mg/

Table 1. Mean concentration of heavy metals (mg/kg, Mean±SD, n=10) in soils from gold mining (SG1, SG2, and SG3) and reference (SGC) sites

Site	As	Cd	Hg	Pb	Ni	Cr	Fe	Co	Cu	Zn	Mn
SG1	1.37±0.42^{a}	6.41±0.62^{a}	6.23±0.70^{a}	29.40±2.40^{a}	29.90±3.1^{a}	57.5±5.5^{a}	46,440.33±419^{a}	26.51±2.3^{a}	44.73±3.2^{a}	160.3±7.4^{a}	1,295.75±18^{a}
SG2	1.35±0.42^{a}	4.77±0.52^{c}	4.69±0.45^{c}	26.16±2.34^{c}	17.69±1.9^{b}	54.35±4.3^{c}	24,966.63±241^{b}	8.60±0.01^{b}	23.40±2.1^{b}	98.84±4.0^{b}	415.94±15^{bc}
SG3	1.25±0.32^{a}	3.46±0.44^{b}	2.77±0.37^{b}	16.43±2.16^{b}	27.78±2.8^{a}	38.35±4.1^{b}	32,639.1±373^{c}	13.72±1.1^{c}	21.81±2.3^{c}	91.98±7.1^{b}	577.15±177^{b}
SGC	0.96±0.24^{b}	0.13±0.02^{d}	1.50±0.26^{d}	8.87±0.31^{d}	12.67±2.5^{c}	18.33±1.5^{d}	3,192.0±73^{d}	12.5±1.2^{c}	7.0±0.8^{d}	123.3±15.3^{c}	301.3±15^{c}
Dutch Target Values	29.00	0.8	0.3	85.00	35.00	100.00	—	—	36.00	140.00	—

Source: Ministry of Housing, Spatial Planning and the Environment (VROM), Dutch Soil Quality Standards (2000), with revisions and updates incorporated in 2009 and 2013

Values are presented as mean ± standard deviation (n = 10). Different superscript letters within a column indicate significant differences among sites (one-way ANOVA followed by Tukey's HSD test, $P < 0.05$). Concentrations are expressed in mg/kg dry weight

Soil quality guideline values are based on Dutch Target Values and are presented for comparative screening purposes only. They do not represent regulatory compliance criteria for the study area

Fe, Co, and Mn were excluded from guideline comparison because no Dutch Target Values are specified for these elements in the selected framework

kg, substantially exceeding the Dutch Target Value for soil quality (0.8 mg/kg) at all investigated mining sites (Table 1). The highest concentration occurred at SG1 (6.41 mg/kg), indicating pronounced Cd enrichment at this site.

Mean Hg concentrations ranged from 1.50 to 6.23 mg/kg, with the highest concentration recorded at SG1 (6.23 ± 0.70 mg/kg) and the lowest one at the comparative reference site (SGC; 1.50 ± 0.26 mg/kg) (Table 1). All mining-impacted sites exhibited Hg concentrations substantially exceeding the Dutch Target Value for soil quality (0.3 mg/kg), indicating considerable Hg enrichment in the studied mining landscape. Likewise, mean Pb concentrations ranged from 8.87 to 29.40 mg/kg, with the highest concentration recorded at SG1 (29.40 ± 2.40 mg/kg) and the lowest concentration at the comparative reference site (SGC; 8.87 ± 0.31 mg/kg) (Table 1). Mining-impacted soils generally exhibited higher Pb concentrations than the reference soil, indicating localized Pb enrichment that may reflect the combined influence of mining activities and site-specific geochemical variability. However, all measured concentrations remained below the Dutch Target Value for soil quality (85 mg/kg), suggesting that Pb contamination was relatively limited compared with the established screening level.

Mean Ni concentrations ranged from 12.67 to 29.90 mg/kg, with the highest concentration recorded at SG1 (29.90 ± 3.10 mg/kg) and the lowest concentration at the comparative reference site (SGC; 12.67 ± 2.50 mg/kg) (Table 1). Mining-affected soils generally exhibited higher Ni concentrations than the reference soil, indicating localized Ni enrichment that may reflect the combined influence of mining disturbance and site-specific geochemical variability. However, all measured concentrations remained below the Dutch Target Value for soil quality (35 mg/kg). Mean Cr concentrations ranged from 18.33 ± 1.50 mg/kg at SGC to 57.50 ± 5.50 mg/kg at SG1 (Table 1). Mining-affected soils showed higher Cr concentrations than the reference soil, indicating localized Cr enrichment that may reflect the combined influence of mining disturbance and geochemical variability. However, all measured concentrations remained below the Dutch Target Value (100 mg/kg). Iron (Fe) was the most abundant element, with concentrations ranging from 3,192.0 ± 73 mg/kg at SGC to 46,440.33 ± 419 mg/kg at SG1.

Mean Co concentrations ranged from 8.60 ± 0.01 mg/kg at SG2 to 26.51 ± 2.30 mg/kg at SG1. The highest concentration at SG1 exceeded the Dutch Target Value (20 mg/kg), indicating localized Co enrichment, whereas concentrations at the other sites remained below the screening value. Similarly, mean Cu concentrations ranged from 7.00 ± 0.80 mg/kg at SGC to 44.73 ± 3.20 mg/kg at SG1 (Table 1). Mining-affected soils generally showed higher Cu concentrations than the reference soil, with SG1 exceeding the Dutch Target Value (36 mg/kg), indicating localized Cu enrichment. Mean Zn concentrations ranged from 91.98 ± 7.10 mg/kg at SG3 to 160.30 ± 7.40 mg/kg at SG1. Zn concentrations varied among sites, and SG1 slightly exceeded the Dutch Target Value (140 mg/kg), whereas the other sites remained below the screening value. Likewise, mean Mn concentrations ranged from 301.30 ± 15 mg/kg at SGC to 1,295.75 ± 18 mg/kg at SG1, demonstrating substantial spatial variability. The highest concentration occurred at SG1, the site most strongly influenced by mining activities, indicating localized Mn enrichment.

Contamination assessment of heavy metals in soils

Contamination factor (CF)

The contamination factor (CF) values for individual heavy metals are presented in Table 2. Overall, CF values followed the order: Hg > Cd > Co > Zn > Mn > Cu > Pb > Fe > Cr > Ni > As.

Across all sites, As (0.19–0.27), Ni (0.32–0.75), and Cr (0.26–0.82) exhibited low contamination ($CF < 1$), indicating limited enrichment relative to the comparative reference site. Moderate contamination ($1 \leq CF < 3$) was observed for Fe (SG1), Co (SG1 and SGC), Cu (SG1), Zn (all sites), Mn (SG1), and Pb (SG1 and SG2), reflecting localized enrichment. In contrast, Cd exhibited very high contamination at all mining sites, while Hg showed very high contamination at every sampling site, including the comparative reference site, indicating widespread Hg enrichment.

Degree of contamination (Cdeg)

The degree of contamination (Cdeg) ranged from 21.04 at the comparative reference site (SGC) to 118.82 at SG1, with values of 84.34 and 58.68 recorded at SG2 and SG3,

respectively (Table 2). According to the classification criteria, all mining sites were classified as having **very** high degrees of contamination, whereas the comparative reference site was classified as considerably contaminated.

Modified degree of contamination (mCdeg)

The modified degree of contamination (mCdeg) ranged from 1.91 at the comparative reference site to 10.80 at SG1, while SG2 and SG3 recorded values of 7.85 and 5.33, respectively (Table 2). Based on the classification criteria, SG1 exhibited very high contamination, SG2 and SG3 exhibited high contamination, and the comparative reference site showed low contamination.

Potential ecological risk factor (ER) and ecological risk index (ERI)

The potential ecological risk factor (ER) and ecological risk index (ERI) values are presented in Table S5. ER values varied substantially among the investigated elements. Cd and Hg showed markedly higher ER values than the other metals, with Cd ranging from 26 to 1,282 and Hg from 600 to 2,492. At all mining sites, Cd exhibited very high ecological risk (ER > 320), while Hg showed very high ecological risk at all sampling sites, including the comparative reference site. In contrast, the remaining metals generally exhibited low ecological risk (ER < 40).

The integrated ecological risk index (ERI) ranged from 642.7 at the comparative reference site to 3,817.5 at SG1, with values of 2,855.3 and 1,825.5 at SG2 and SG3, respectively. According to Hakanson's classification, all sampling sites fell within the very high ecological risk category (ERI ≥ 600), with SG1 showing the highest overall ecological risk.

Pollution load index (PLI)

The Pollution Load Index (PLI) values are presented in Figure 2. PLI values were 2.48 at SG1, 1.54 at SG2, 1.49 at SG3, and 0.59 at the comparative reference site (SGC) (Figure 2). According to the PLI classification, values > **1** indicate pollution, whereas values < **1** indicate no overall pollution. Accordingly, all mining sites were classified as polluted, with SG1 exhibiting the highest pollution load, whereas the comparative reference site reflected background conditions. Overall, the PLI assessment corroborates the contamination and ecological risk indices, identifying SG1 as the most impacted site, followed by SG2 and SG3, while the comparative reference site reflected background soil conditions.

Sensitivity considerations

The choice of reference values influences contamination factor (CF), enrichment factor (ER), and ecological risk index (ERI) calculations. Metals with low natural variability, such as Cd and Hg, consistently indicated very high contamination, regardless of whether global or local reference values were used. In contrast, metals with higher natural variability, including Fe and Cr, could yield substantially different CF values if local or geologic baselines exceed global averages (e.g., CF_Fe 1.20 → 1.03; CF_Cr 2.5 → 1.9; CF_Cd 12.0 → 12.0; CF_Hg 8.0 → 8.0), with ER and ERI showing similar patterns. The corresponding changes in CF values and contamination classifications under alternative background assumptions are summarized in Table S6.

Multivariate analyses of heavy metals in gold mining-impacted soils

Correlation analysis among heavy metals

Pearson's correlation analysis was performed to evaluate relationships among heavy metals and identify similarities in their distribution patterns in gold-mining-impacted soils. The correlation matrix (Figure 3; Table S7) revealed predominantly positive relationships among the investigated elements, with several statistically significant correlations ($P < 0.05$ and $P < 0.01$), indicating similarities in their spatial variability and possible common controlling processes.

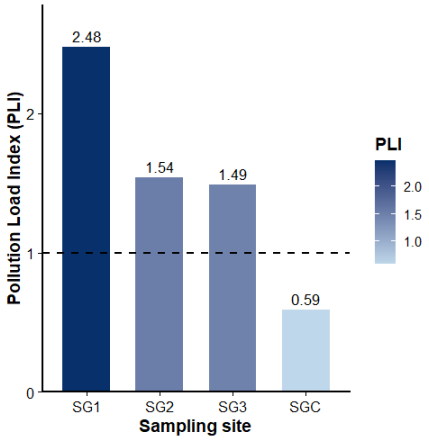


Figure 2. Spatial variation of Pollution Load Index (PLI) for heavy metals in soils from the Osole gold mining area. The color gradient represents differences in PLI magnitude among sampling sites, and the dashed line indicates the threshold value (PLI = 1)

Table 2. Contamination factor (CF), degree of contamination (Cdeg), and modified degree of contamination (mCdeg) of heavy metals for soil from gold mining (SG1, SG2, and SG3) and the reference (SGC) sites

Site	Contamination factor (CF)											C_d	Cdeg	mCdeg	Status
	As	Cd	Hg	Pb	Ni	Cr	Fe	Co	Cu	Zn	Mn				
SG1	0.27	**42.73**	**62.3**	1.73	0.75	0.82	1.33	2.65	1.79	2.29	2.16	118.82	Very high	10.80	Very high
SG2	0.27	**31.80**	**46.9**	1.54	0.44	0.78	0.71	0.86	0.94	1.41	0.69	84.34	Very high	7.85	High
SG3	0.25	**23.07**	**27.7**	0.97	0.70	0.55	0.93	1.37	0.87	1.31	0.96	58.68	Very high	5.33	High
SGC	0.192	0.87	**15.0**	0.52	0.32	0.26	0.09	1.25	0.28	1.76	0.50	21.04	Considerable	1.91	Low

Bold values of the contamination factor (CF) indicate values greater than 6, corresponding to a very high level of soil contaminatio

Strong positive associations were observed among several elements, particularly Cd, Hg, Pb, Cr, Fe, and Cu. Cd showed strong correlations with Hg, Pb, Cr, Fe, and Cu (r = 0.922–0.930, $P < 0.01$). Similarly, Hg was strongly correlated with Pb, Cu, and Cr (r = 0.887–0.933, $P < 0.01$), while Fe showed strong associations with Cu, Ni, and Mn (r = 0.850–0.936, $P < 0.01$). These relationships indicate similar spatial distribution patterns and may reflect shared controlling processes, including mining-related disturbance, mobilization, and redistribution of metal-bearing materials. However, strong correlations do not by themselves establish a common contamination source and may also arise from similarities in mineralogical composition, soil retention mechanisms, and physicochemical behavior.

Nickel exhibited intermediate to strong associations with Fe (r = 0.891), Cu (r = 0.762), Mn (r = 0.755), and Cd (r = 0.696), suggesting that its distribution may be influenced by both shared geochemical controls and mining-related processes. A distinct association was also observed among Co, Zn, and Mn, with strong correlations between Co–Zn (r = 0.867), Co–Mn (r = 0.923), and Zn–Mn (r = 0.753) ($P < 0.01$). These relationships suggest that these elements may share controlling factors related to mineralogical composition, soil properties, or anthropogenic inputs. In contrast, As showed comparatively weaker relationships with most metals, with moderate correlations with Hg (r = 0.573), Cd (r = 0.464), Pb (r = 0.403), Cr (r = 0.407), and Fe (r = 0.412). Its correlations with Zn (r = 0.046) and Co (r = 0.154) were not significant, suggesting that As may follow a distinct distribution pattern related to differences in mineral association and mobility.

Principal component analysis of heavy metals

Principal component analysis (PCA) with Varimax rotation was performed to evaluate relationships among eleven heavy metals and identify the dominant factors controlling their variability in gold mining-impacted soils. The suitability of the dataset was confirmed by the Kaiser–Meyer–Olkin (KMO) value (0.852) and Bartlett's test of sphericity ($\chi^2 = 802.236$, df = 55, $P < 0.001$), indicating adequate sampling and a suitable correlation matrix for factor extraction.

Two principal components with eigenvalues > 1 were extracted, explaining 85.0% of the total variance in heavy metal concentrations (Table S8; Figure 4). After Varimax rotation, PC1 accounted for 50.061% of the variance, while PC2 explained 34.938%, indicating that these components captured the major correlation structures among the investigated elements.

Principal component analysis (PCA) revealed that PC1 accounted for 69.879% of the total variance and exhibited strong positive loadings for Cr (0.931), Cd (0.912), Pb (0.898), Hg (0.873), Fe (0.797), and Cu (0.762), with moderate contributions from As (0.624) and Ni (0.554). PC2 explained 15.120% of the total variance and was characterized by strong positive loadings for Co (0.953), Zn (0.927), and Mn (0.836), together with moderate contributions from Cu (0.632), Ni (0.568), and Fe (0.520). Arsenic exhibited a distinct loading pattern, with a moderate positive loading on PC1 (0.624) and a negligible loading on PC2 (–0.053).

Hierarchical cluster analysis of heavy metals

Hierarchical cluster analysis (HCA) was performed on standardized heavy metal concentrations using Ward's minimum variance method (Ward.D2) with Euclidean distance to evaluate similarities among elements and support PCA-derived associations (Figure 5). The dendrogram revealed distinct groups of Heavy metals with comparable variability patterns in gold mining-impacted soils. A major cluster consisted of Cd, Hg, Pb, Cr, Fe, and Cu, showing strong agreement with elements exhibiting high positive loadings on PC1. Arsenic exhibited a relatively close association with this group, consistent with its moderate contribution to PC1; however, its distinct position suggests that additional geochemical processes

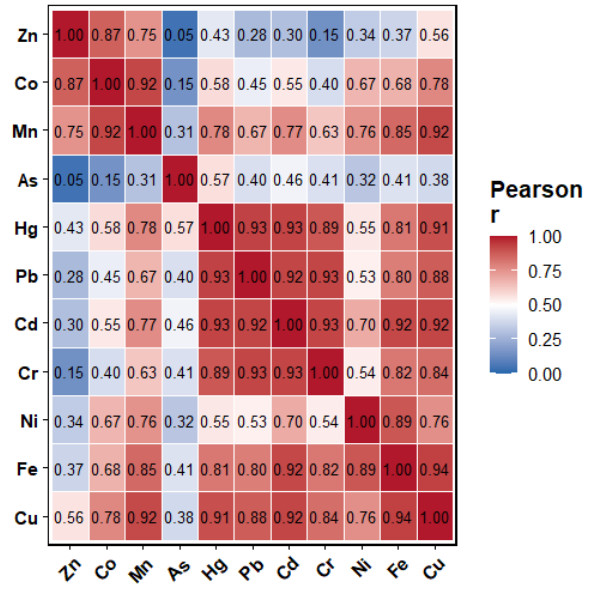


Figure 3. Pearson's correlation heatmap with hierarchical clustering of heavy metals in gold mining-impacted soils from the Osole area. The color gradient indicates the magnitude of correlation coefficients (r), and clustering patterns highlight elemental associations consistent with multivariate analyses

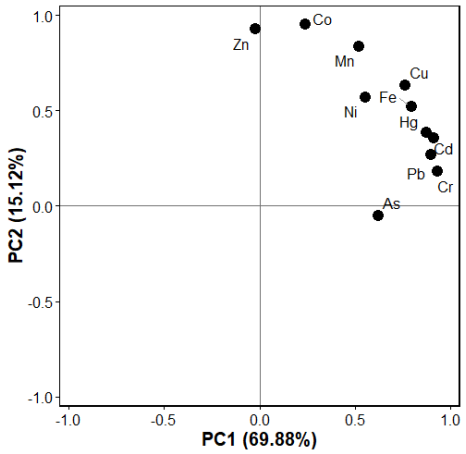


Figure 4. Principal component analysis (PCA) loading plot illustrating the contribution and associations of heavy metals along the first two principal components (PC1 and PC2) in gold mining-impacted soils at Osole

may influence its behavior.

A second cluster was mainly composed of Co, Zn, and Mn, corresponding well with their strong positive loadings on PC2. Ni showed an intermediate position, consistent with its moderate contributions to both PC1 and PC2, indicating that its variability may be controlled by multiple interacting processes.

Human health risks of heavy metals in soils

Non-carcinogenic risk (HQ and HI)

The potential non-carcinogenic health risks associated with exposure to heavy metals in soils from gold-mining areas were evaluated using the hazard quotient (HQ) and hazard index (HI) approaches. HQ values were calculated for individual elements and exposure pathways, including soil ingestion, dust inhalation, and dermal contact. The total hazard index (THI) was calculated by summing HQ values across all investigated elements and exposure pathways to characterize cumulative exposure. This approach assumes additive effects among contaminants and exposure routes. Under the commonly applied risk-assessment framework, HQ or HI values below 1.0 indicate that adverse health effects are unlikely under the assumed exposure conditions, whereas values exceeding 1.0 indicate potential non-carcinogenic health concerns requiring further evaluation.

All individual HQ values for children and adults remained below 1.0 across all exposure pathways (Tables S9–S14), indicating that no individual metal exceeded the screening benchmark when assessed independently. However, cumulative exposure to multiple metals resulted in elevated THI values among children at the mining sites. As shown in Table 3, THI values for children were 2.62, 1.51, and 1.53 at SG1, SG2, and SG3, respectively, exceeding the screening value of 1.0. These results indicate potential cumulative non-carcinogenic health concerns under the modeled exposure conditions. In contrast, the comparative reference site (SGC) had a THI of 0.51, indicating a lower cumulative exposure burden under the same assessment framework. Fe, Mn, Cr, and Hg were the major contributors to children's cumulative exposure index. At SG1, Fe had the highest HQ (0.93), followed by Mn (0.77), Cr (0.29), and Hg (0.29). Fe and Mn together accounted for approximately 65% of the total THI at this site.

Exposure-pathway analysis demonstrated that soil ingestion was the dominant contributor to cumulative exposure among children, whereas dust inhalation and dermal contact contributed comparatively little. At SG1, soil ingestion accounted for approximately 95% of the total THI (2.45 of 2.62), while inhalation and dermal pathways contributed only minor proportions.

For adults, THI values were considerably lower than those observed for children and remained below the screening benchmark at all investigated sites (Table 4). THI values were 0.34, 0.20, 0.20, and 0.07 at SG1, SG2, SG3, and SGC, respectively, indicating no cumulative non-carcinogenic concern above the screening benchmark under the evaluated exposure conditions. Similar to children, Fe, Mn, Cr, and Hg were the major contributors to adult cumulative exposure, with the highest HQ values at SG1 observed for Fe (0.123), Mn (0.100), Cr (0.038), and Hg (0.037).

Carcinogenic risk assessment (CR and TCR)

The carcinogenic risks associated with exposure to heavy metals in soils from gold-mining areas were evaluated using carcinogenic risk (CR) and total cancer risk (TCR). CR was calculated for individual elements and exposure pathways, including soil ingestion, dust inhalation, and dermal contact, whereas TCR represented the cumulative carcinogenic risk across the investigated exposure pathways (Table S15 –S20). According to USEPA risk-assessment guidelines, an excess lifetime cancer risk in the range of 10^{-6} to 10^{-4} is generally considered acceptable, whereas values exceeding 1.0×10^{-4} indicate potential carcinogenic concern requiring further evaluation.

For children, Ni- and Cr-specific CR values and the

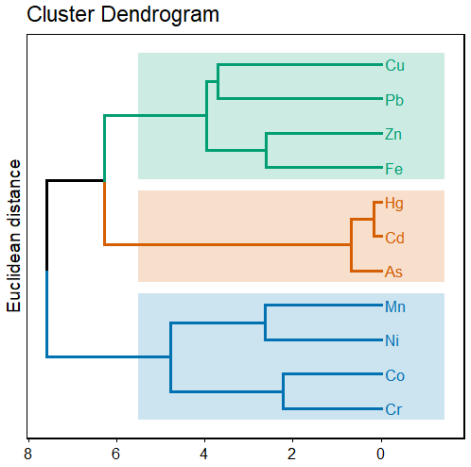


Figure 5. Hierarchical cluster analysis (HCA) dendrogram of heavy metals in soils affected by gold mining activities at Osole. Metal clustering was performed using standardized concentrations, Euclidean distance, and Ward's minimum variance method (Ward.D2), highlighting similarities in elemental variability and distribution patterns

Table 3. Combined Hazard Quotient (CHQ) and Total Hazard Index (THI) of Heavy metals in soils for children at SG1, SG2, SG3, and the comparative reference site (SGC)

Site	Combined Hazard Quotient (CHQ)											Total Hazard Index (THI)
	As	Cd	Hg	Pb	Ni	Cr	Fe	Co	Cu	Zn	Mn	
SG1	6.09×10^{-2}	1.09×10^{-1}	2.88×10^{-1}	1.14×10^{-1}	2.13×10^{-2}	2.92×10^{-1}	9.31×10^{-1}	8.46×10^{-3}	1.50×10^{-2}	7.14×10^{-3}	7.71×10^{-1}	**2.60**
SG2	6.04×10^{-2}	8.14×10^{-2}	2.17×10^{-1}	1.02×10^{-1}	1.26×10^{-2}	2.75×10^{-1}	5.00×10^{-1}	2.74×10^{-3}	7.82×10^{-3}	4.41×10^{-3}	2.48×10^{-1}	**1.50**
SG3	5.57×10^{-2}	5.91×10^{-2}	1.28×10^{-1}	6.37×10^{-2}	1.98×10^{-2}	1.94×10^{-1}	6.54×10^{-1}	4.38×10^{-3}	7.29×10^{-3}	4.10×10^{-3}	3.44×10^{-1}	**1.51**
SGC	4.28×10^{-2}	2.22×10^{-3}	6.93×10^{-2}	3.44×10^{-2}	9.04×10^{-3}	9.29×10^{-2}	6.40×10^{-2}	3.99×10^{-3}	2.34×10^{-3}	5.50×10^{-3}	1.79×10^{-1}	0.58

Values in bold (>1) indicate potential non-carcinogenic health risk

overall TCR values exceeded 1.0×10^{-4} at all investigated sites, including the comparative reference site (SGC) (Table 5). TCR values were 1.18×10^{-3}, 7.50×10^{-4}, 9.80×10^{-4}, and 4.52×10^{-4} at SG1, SG2, SG3, and SGC, respectively, indicating elevated estimated lifetime cancer risk under the modeled exposure scenarios. Ni and Cr were the principal contributors to the estimated carcinogenic risk in children. Ni produced the highest CR values, reaching 7.24×10^{-4}, 4.29×10^{-4}, 6.74×10^{-4}, and 3.07×10^{-4} at SG1, SG2, SG3, and SGC, respectively, followed by Cr, with corresponding values of 3.88×10^{-4}, 2.66×10^{-4}, 2.60×10^{-4}, and 1.24×10^{-4}.

For adults, individual CR values remained below 1.0×10^{-4} at all sites (Table S21). However, cumulative exposure resulted in TCR values above this threshold at SG1 (1.41×10^{-4}), SG2 (1.03×10^{-4}), and SG3 (1.17×10^{-4}), whereas SGC remained below the threshold (5.17×10^{-5}). As observed for children, Ni and Cr were the principal contributors to adult carcinogenic risk. Ni showed the highest CR values, followed by Cr, indicating that these two elements made the largest contributions to the modeled cumulative cancer risk.

Exposure pathway analysis showed that soil ingestion was the predominant contributor to the modeled carcinogenic risk for both children and adults, whereas dust inhalation and dermal contact contributed relatively small proportions. At SG1, for example, soil ingestion accounted for approximately 95% of children's TCR and approximately 99% of adults' TCR.

Discussion

Concentration of heavy metals in soils

These exceedances indicate localized enrichment of specific heavy metals and identify Cd and Hg as priority elements requiring further environmental assessment in the study area (Table 1). The observed spatial variability in heavy metal concentrations likely reflects the combined influence of mining-derived inputs, geological background, and soil physicochemical characteristics. Mining-affected soils exhibited lower organic matter content (1.16–3.07%) and cation exchange capacity (CEC) compared with the reference soil (OM = 12.94%), which may reduce metal retention capacity and influence heavy metal mobility (Table S4). In addition, the neutral to alkaline soil conditions observed in the study area may regulate heavy metal behavior through adsorption, precipitation, and mineral-surface interactions. Overall, heavy metal distribution in the Osole gold-mining area reflects the complex interaction among anthropogenic disturbance, geological characteristics, and soil geochemical processes.

The observed As concentrations were relatively low compared with those reported from other gold-mining regions, including the Adola gold-mining area in Ethiopia (59.7 mg/kg), Meli in Tigray (13.0 mg/kg), and mining-affected soils in Ghana, Nigeria, and China (3,4,6,8,9). The relatively low As concentrations in the present study (Table 1) suggest that As was not a major contributor to the overall contamination burden. However, total As concentrations alone cannot establish its environmental mobility or toxicity because these properties depend on chemical speciation, mineral associations, and bioavailability. In particular, inorganic As species such as As(III) and As(V) differ in mobility and toxicity. Therefore, future investigations incorporating As speciation and bioavailability assessments would provide a more comprehensive evaluation of the environmental significance of As in the study area.

The elevated Cd concentrations may be associated with mining and gold-processing activities, including mine-waste accumulation and the mobilization of Cd-bearing mineral materials (Table 1). In addition, the relatively low organic matter content and cation exchange capacity (CEC)

Table 4. Combined Hazard Quotient (CHQ) and Total Hazard Index (THI) of heavy metals in soils for adults at SG1, SG2, SG3, and the comparative reference site (SGC)

Site	Combined Hazard Quotient (CHQ)											Total Hazard Index (THI)
	As	Cd	Hg	Pb	Ni	Cr	Fe	Co	Cu	Zn	Mn	
SG1	7.62×10^{-3}	1.49×10^{-2}	3.66×10^{-2}	1.44×10^{-2}	2.74×10^{-3}	3.84×10^{-2}	1.23×10^{-1}	1.15×10^{-3}	1.87×10^{-3}	8.94×10^{-4}	9.96×10^{-2}	0.33
SG2	7.64×10^{-3}	1.11×10^{-2}	2.75×10^{-2}	1.28×10^{-2}	1.62×10^{-3}	3.63×10^{-2}	6.59×10^{-2}	3.74×10^{-4}	9.79×10^{-4}	5.51×10^{-4}	3.20×10^{-2}	0.20
SG3	7.00×10^{-3}	8.06×10^{-3}	1.63×10^{-2}	8.03×10^{-3}	2.55×10^{-3}	2.56×10^{-2}	8.82×10^{-2}	5.96×10^{-4}	9.12×10^{-4}	5.13×10^{-4}	4.44×10^{-2}	0.20
SGC	5.36×10^{-3}	3.03×10^{-4}	8.81×10^{-3}	4.34×10^{-3}	1.16×10^{-3}	1.22×10^{-2}	8.43×10^{-3}	5.43×10^{-4}	2.93×10^{-4}	6.88×10^{-4}	2.32×10^{-2}	0.07

Values in bold (>1) indicate potential non-carcinogenic health risk

Table 5. Carcinogenic Risk (CR) of Heavy metals for Children through Soil Exposure at SG1, SG2, SG3, and the Comparative reference site (SGC)

Site	Carcinogenic Risk (CR)					Total Lifetime Cancer Risk (TCR)
	As	Cd	Pb	Ni	Cr	
SG1	2.75×10^{-5}	3.26×10^{-5}	3.34×10^{-6}	**7.24×10^{-4}**	**3.88×10^{-4}**	**1.18×10^{-3}**
SG2	2.71×10^{-5}	2.43×10^{-5}	2.97×10^{-6}	**4.29×10^{-4}**	**2.66×10^{-4}**	**7.50×10^{-4}**
SG3	2.51×10^{-5}	1.75×10^{-5}	1.87×10^{-6}	**6.74×10^{-4}**	**2.60×10^{-4}**	**9.80×10^{-4}**
SGC	1.93×10^{-5}	1.01×10^{-6}	1.01×10^{-6}	**3.07×10^{-4}**	**1.24×10^{-4}**	**4.52×10^{-4}**

Values in bold (>1.0 x 10^{-4}) indicate potential carcinogenic health risk

Note: Values in bold (>1.0×10^{-4}) indicate potential carcinogenic health risk. Cancer risk estimates were calculated based on total metal concentrations and assume that 100% of the measured element is present in its carcinogenic form (e.g., Cr as Cr(VI)). Therefore, these estimates should be interpreted as conservative and may overestimate the actual carcinogenic risk where non-carcinogenic species (e.g., Cr(III)) are present

of the mining soils may reduce Cd retention and thereby enhance its mobility. Compared with previous studies, Cd concentrations in the present study were higher than those reported for Ethiopian agricultural soils from Ziway (0.0783 mg/kg) and Bole Lemi Industrial Park (1.0 mg/kg) (12,33), but lower than concentrations reported for highly contaminated gold-mining environments such as Pawara, Cameroon (9.09–25.0 mg/kg), Nangodi, Ghana (8.78 mg/kg), and other global mining soils (23.24 mg/kg) (4,7,32). The concentrations were comparable to those reported from Zamfara State, Nigeria (6.81 mg/kg) but higher than those reported for Chinese gold-mining soils (0.3554 mg/kg) (6,8). These differences among mining areas may reflect variations in ore characteristics, mining intensity, waste-management practices, and local soil properties. Overall, the consistent exceedance of the Dutch Target Value identifies Cd as a priority contaminant in the Osole gold-mining area and supports its consideration in subsequent ecological and human-health risk assessments.

The elevated Hg concentrations are consistent with the potential influence of artisanal and small-scale gold-mining (ASGM) activities, particularly mercury amalgamation, ore processing, amalgam burning, and disposal of Hg-contaminated wastes (Table 1). Compared with previous studies, Hg concentrations in the present study were higher than those reported in irrigated horticultural soils from Ziway, Ethiopia (1.96 mg/kg) (12), and were within the range reported for gold-mining environments in Burkina Faso (3.83 mg/kg) and Ghana (3.9–7.5 mg/kg) (4,34). The maximum concentration at SG1 (6.23 mg/kg) also exceeded the global mean reported for gold-mining soils (3.58 mg/kg) (32), highlighting Hg as an important contaminant of concern in the Osole mining area. However, because the present study measured total Hg, the results do not distinguish among different Hg species or directly establish the contribution of individual Hg sources. Moreover, the air-drying step used during sample preparation may have caused some Hg volatilization, and we could not quantify any potential loss because we did not analyze paired wet- and air-dried samples. Therefore, the reported Hg concentrations should be interpreted with this analytical uncertainty in mind. The environmental behavior and toxicity of Hg also depend strongly on its chemical form, mobility, and transformation processes, including methylmercury formation under favorable environmental conditions. Future investigations incorporating Hg speciation, bioavailability, and validated moisture-preserving sample preparation would provide a more comprehensive assessment of Hg exposure pathways and long-term environmental risks.

Compared with previous studies, Pb concentrations in the present study (Table 1) were comparable to those reported from the Hawassa Industrial Zone (28.7 mg/kg), Ziway agricultural soils (30.9 mg/kg), and Legadembi gold-mine tailings (19.0–40.0 mg/kg) (3,11,12). The observed concentrations were higher than those reported from Nangodi, Ghana (11.71 mg/kg) and Bissa, Burkina Faso (17.94 mg/kg) (4,34). These differences may reflect variations in mining intensity, ore characteristics, geological background, and soil properties. Although Pb concentrations remained below the Dutch Target Value, the persistence of Pb and its potential mobility and bioavailability warrant consideration in long-term environmental risk assessments.

The observed Ni concentrations (Table 1) were substantially lower than those reported from the Adola gold-mining area, Ethiopia (224.7 mg/kg), but higher than values reported from Dale Woreda, Sidama (6.53 mg/kg) and Ziway agricultural soils (0.194 mg/kg) (9,12,35). Compared with other gold-mining regions, Ni concentrations in the present study were lower than those reported from Bissa, Burkina Faso (38.87 mg/kg) and Chinese gold-mining soils (30.6 mg/kg), but higher than values reported from Zamfara, Nigeria (1.25–6.36 mg/kg) (6,8,34). These differences may reflect variations in ore characteristics, mining intensity, geological background, and soil properties. Although Ni concentrations remained below the Dutch Target Value, the observed spatial enrichment warrants consideration of Ni mobility and bioavailability in future environmental assessments.

The observed Cr concentrations (Table 1) were higher than those reported from several Ethiopian soils (33,36), but lower than those reported from highly contaminated gold-mining areas such as Pawara, Cameroon (7). The spatial variability of Cr may reflect interactions among mining-related inputs, Cr-bearing minerals, and geological background. Because Cr toxicity depends strongly on its chemical form, particularly its oxidation state, future studies incorporating Cr speciation would provide a more robust assessment of its potential environmental significance.

The predominance of Fe is consistent with its strong lithogenic contribution and its role in the mineral matrix of soils. Compared with other mining environments, Fe concentrations (Table 1) were higher than those reported from several African gold-mining areas but lower than those reported from some Ethiopian soils developed from Fe-rich parent materials (4,8,36). The spatial distribution of Fe likely reflects natural mineralogical and geological variability, with possible localized influence from mining disturbance. Therefore, the elevated Fe concentrations should not be interpreted as evidence of anthropogenic contamination alone.

The elevated Co concentration at SG1 may reflect the combined influence of mining activities, mineral composition, and local geochemical conditions. Because Co distribution can be strongly influenced by parent materials and mineral associations, further mineralogical characterization would help distinguish potential anthropogenic enrichment from natural geochemical variability.

The observed concentrations were comparable with those reported from Ethiopian and other gold-mining environments (6,10,11). The spatial distribution of Cu may reflect the combined influence of mining-related inputs, Cu-bearing minerals, and soil properties, identifying SG1

as a site warranting further assessment.

Compared with previous studies, the Zn concentrations observed in the present study (Table 1) were higher than those reported for several agricultural and mining-affected soils but remained within the ranges reported for some gold-mining environments (6,8,11). The spatial variability of Zn, including the lower concentrations at SG2 and SG3, suggests that its distribution may be controlled by a combination of geological factors, soil properties, and mining-related processes.

The observed Mn concentrations (Table 1) were comparable with those reported from gold-mining regions globally (32) and higher than several Ethiopian soils (35,36). However, because Mn is naturally abundant in many geological settings, the observed enrichment should be interpreted in the context of mineralogical composition, parent material, and other geochemical controls rather than attributed solely to mining activities.

Overall, the heavy metal distribution demonstrates a clear spatial contrast between the mining-impacted sites and the comparative reference site. SG1 consistently exhibited the highest concentrations of most elements, including Cd, Hg, Pb, Ni, Cr, Fe, Co, Cu, and Mn, whereas SG2 and SG3 generally showed intermediate concentrations. This spatial pattern suggests a localized enrichment gradient associated with proximity to mining and processing activities. The particularly pronounced enrichment of Cd and Hg distinguishes these elements from the predominantly lithogenic elements Fe, Mn, and Cr, indicating that both anthropogenic inputs and geochemical background contribute to the observed heavy metal distribution. The elevated concentrations at SG1, combined with the progressive differences among downstream sites, further suggest that contaminant distribution is spatially heterogeneous rather than uniform across the mining landscape.

Contamination assessment of heavy metals in soils

Contamination factor (CF)

The exceptionally high CF values for Cd and Hg identify these elements as the dominant contributors to the observed contamination (Table 2). Their enrichment may be associated with mining-related inputs and accumulation in soils, whereas the relatively low CF values for As, Ni, and Cr indicate limited enrichment. Compared with previous studies from Ethiopia and other African mining regions, the CF values for Cd and Hg were generally higher, suggesting comparatively greater contamination in the investigated gold-mining area (3,7,8,12). Similar enrichment patterns have been reported in mining-impacted environments, where ore extraction and processing can increase metal accumulation in soils (37,38).

The substantially higher Cdeg values at the mining sites indicate cumulative contamination by multiple heavy metals rather than enrichment by individual elements alone (Table 2). The highest **Cdeg** value at SG1 was largely driven by elevated CF values for Cd, Hg, Co, Zn, Mn, Cu, and Fe, indicating a greater cumulative contamination burden at this site. Compared with previous studies in Ethiopia and other African mining regions, the Cdeg values obtained in this study were considerably higher, demonstrating a greater overall contamination burden (3,12,34).

Unlike the Cdeg index, mCdeg normalizes contamination by the number of analyzed elements, providing a more balanced assessment of overall soil contamination. The elevated mCdeg values indicate cumulative enrichment across multiple metals rather than enrichment restricted to a single element (Table 2). The high mCdeg values were largely driven by the exceptionally high CF values of Cd and Hg, highlighting their dominant contribution to overall soil contamination. Similar observations have been reported for mining-affected soils, where cumulative contamination indices help distinguish elevated metal enrichment from background geochemical conditions (3,37).

The exceptionally high ER values for Cd and Hg reflect the combined effects of their elevated contamination factors and high toxic-response coefficients in the Hakanson ecological risk model (Table S8). Consequently, these two elements were the dominant contributors to ecological risk in the study area. Although Co, Zn, Cu, and Pb showed varying degrees of enrichment, their lower toxic-response coefficients resulted in comparatively smaller contributions to the overall ecological risk. Similar patterns have been reported in mining-impacted environments, where Cd and Hg frequently contribute disproportionately to ecological risk because of their toxicity and persistence (3,7,12,38).

The elevated ERI values were predominantly driven by Cd and Hg, indicating that these two elements accounted for most of the integrated ecological risk despite the relatively low ER values of the other metals (Table S8). Because air-drying may have resulted in Hg volatilization and consequently underestimated total Hg concentrations, the calculated ER and ERI values associated with Hg should be considered conservative lower-bound estimates of the potential ecological risk. Compared with previous studies from Ethiopia and other mining regions, the ERI values observed in the present study indicate a comparatively high ecological risk burden, highlighting the potential environmental significance of metal contamination in the studied gold-mining area (3,7,12).

Overall, the ecological risk assessment identifies Cd and Hg as the principal ecological risk drivers in the investigated mining area. Their high ER values and dominant contributions to the ERI indicate that these elements warrant priority in future monitoring and environmental management. Future investigations incorporating metal speciation, bioavailability, ecological exposure pathways, and biological response indicators would provide a more comprehensive assessment of the long-term ecological implications of metal contamination associated with gold mining.

In this study, "natural variability" refers to spatial variation in the background concentrations of elements arising from differences in parent material, mineralogical composition, weathering intensity, and other geochemical processes, rather than variation in chemical speciation.

This distinction is important because contamination indices such as CF, ER, and ERI depend on the selected background reference values. Elements such as Fe and Cr commonly exhibit greater lithogenic variability than Cd and Hg; therefore, their contamination indices should be interpreted cautiously where local geological background values are unavailable.

The elevated PLI values indicate cumulative enrichment of heavy metals in mining-affected soils rather than contamination by individual elements alone. The highest PLI at SG1 is consistent with its elevated CF, Cd, mCd, and ERI values, confirming greater anthropogenic influence at this site (Figure 2). Although the PLI integrates contamination from all analyzed elements, the exceptionally high contamination and ecological risk associated with Cd and Hg indicate that these elements were the primary contributors to the observed pollution. Similar relationships between elevated PLI values and Cd–Hg enrichment have been reported in other mining-impacted environments (39).

Overall, the PLI assessment corroborates the contamination and ecological risk indices, identifying SG1 as the most impacted site, followed by SG2 and SG3, while the comparative reference site reflected background soil conditions.

Integrated contamination and ecological-risk interpretation

The contamination and ecological-risk indices provide convergent evidence that Cd and Hg are the principal environmental concerns in the Osole mining area. Their importance is not attributable solely to their absolute concentrations but results from the combination of elevated concentrations relative to the reference background and their high toxic-response coefficients in the Hakanson model. Consequently, Cd and Hg generated exceptionally high contamination factors and ecological risk factors, which in turn dominated the overall ERI values. This relationship is particularly evident at SG1, where the highest Cd and Hg concentrations coincided with the highest CF, mCd, ER, ERI, and PLI values. The consistency among these independent indicators strengthens the interpretation that SG1 represents the principal contamination hotspot.

In contrast, elements such as Fe, Cr, Ni, Zn, Cu, and Mn contributed substantially to total elemental abundance but generally made smaller contributions to ecological risk because of their lower contamination factors and/or lower toxic-response coefficients. This distinction is important because high concentration does not necessarily translate into high ecological risk. For example, Fe was the most abundant element in the soils, yet it was not a major ecological-risk driver, whereas Hg occurred at much lower concentrations but generated extremely high ecological risk. Therefore, concentration-based assessment alone would underestimate the environmental significance of Hg and Cd in the study area.

The agreement between concentration patterns, contamination indices, and ecological-risk indices indicates that the environmental significance of the Osole contamination is driven primarily by Cd and Hg, while the remaining elements provide evidence of broader geochemical and mining-related alteration. This integrated interpretation identifies Cd and Hg as priority contaminants for environmental monitoring and risk management and SG1 as the principal priority area for intervention.

These observations emphasize that while global background values provide a standardized benchmark, interpretation of contamination indices for metals with highly variable natural backgrounds should be approached with caution. Nevertheless, the overall assessment of high contamination at gold mining sites, particularly for Cd and Hg, remains robust.

Multivariate analyses of heavy metals in gold mining-impacted soils

Correlation analysis among heavy metals

The observed correlation patterns (Figure 3) are broadly consistent with previous studies from mining-impacted environments. Weleabzgi et al. (10) reported a strong Cu–Pb correlation ($r = 0.96$) in sediments from artisanal gold-mining areas in Meli, Tigray, Ethiopia. Similarly, Barde et al. (8) and Osei-Akoto et al. (4) reported significant associations among Cd, Pb, Ni, Cr, and Fe in soils affected by gold-mining activities in Nigeria and Ghana, respectively. These similarities suggest that mining disturbance can produce comparable patterns of metal co-occurrence through the mobilization and redistribution of metal-bearing materials.

Nevertheless, differences among studies may result from variations in ore composition, mining practices, waste-management practices, and local soil characteristics. Therefore, Pearson's correlation analysis alone cannot establish common contamination sources. PCA and HCA were subsequently applied to further evaluate dominant metal associations and identify groups of elements with similar distribution patterns.

Principal component analysis

The close association among Cd, Hg, Pb, Cr, and Fe (Figure 4) indicates similar spatial variability, suggesting that these elements are influenced by common controlling processes within the studied soils. Considering the occurrence of artisanal and small-scale gold mining (ASGM) activities in the study area, PC1 may partly reflect mining-related inputs and their effects on soil geochemistry. However, the substantial loadings of Fe and As also indicate the influence of mineralogical composition and natural pedogenic processes. Therefore, PC1 is interpreted as a mixed factor representing both anthropogenic inputs and intrinsic soil geochemical characteristics rather than a single contamination source. The close association of these elements suggests similar variability patterns and potentially common controlling processes, which may reflect the influence of mining-related inputs together with inherent soil geochemical characteristics.

The association of Co, Zn, and Mn forms a geochemically distinct grouping from that observed for PC1, suggesting differences in elemental behavior, mineral associations, and soil properties. This grouping indicates contrasting elemental behavior and suggests the influence of different mineralogical affinities or soil-related processes compared with the PC1-associated elements. The moderate loadings of Cu, Ni, and Fe on both components indicate that these elements are influenced by multiple processes, including both natural geochemical variability and anthropogenic activities.

Arsenic exhibited a distinct loading pattern, with a moderate positive loading on PC1 (0.624) and a negligible loading on PC2 (−0.053), indicating that its variability is largely independent of the elemental association represented by the second component. This pattern may reflect differences in mineralogical occurrence, adsorption–desorption reactions, redox-sensitive transformations, and mobility within the soil environment, suggesting that As is controlled by geochemical processes distinct from those influencing Co, Zn, and Mn.

Overall, the PCA results indicate that heavy metal variability in gold mining-impacted soils is controlled by multiple interacting factors. PC1 represents the dominant correlation structure involving Cd, Hg, Pb, Cr, Fe, and related elements, whereas PC2 reflects a separate association dominated by Co, Zn, and Mn. These findings agree with previous studies demonstrating that multivariate statistical approaches are useful for identifying groups of co-occurring elements in mining-affected environments.

The agreement among correlation analysis, PCA, and HCA demonstrates consistent elemental associations within the studied soils. Nevertheless, these multivariate techniques identify statistical relationships among elements rather than definitive contamination sources. Therefore, interpretation of heavy metal origins requires integration with enrichment factors, contamination indices, mineralogical characterization, ecological risk assessment, and field observations.

Nevertheless, PCA identifies patterns of covariance among variables rather than definitive pollution sources. Consequently, distinguishing lithogenic from anthropogenic contributions requires supporting evidence from geological information, land-use history, enrichment factors, contamination indices, or isotopic analyses.

Differences between the observed clustering patterns and previous studies may reflect variations in geological background, environmental conditions, anthropogenic activities, and land-use characteristics. Samuel et al. (3) reported Cu–Cr and Cd–As–Ni–Pb associations in soils from the Hawassa Industrial Zone, whereas Girma (12) identified different groupings involving As, Cd, Ni, Zn, Cr, and Hg. These variations highlight the site-specific nature of heavy metal associations and their controlling mechanisms. However, PCA identifies statistical relationships rather than definitive sources; therefore, interpretation should be integrated with contamination indices, ecological risk assessment, mineralogical information, and field observations (37,38).

Human health risks of heavy metals in soils

Non-carcinogenic risk (HQ and HI)

Although Fe is an essential element and its elevated concentration may partly reflect the natural geological conditions of the study area, its inclusion in the conservative HQ/HI framework can substantially influence the calculated THI. Other metals, including Hg, Cr, Cd, and Pb, also warrant consideration because of their established toxicological effects (Table 3). Children may represent a more sensitive receptor group because of their higher soil ingestion rates and lower body weight relative to adults. This finding highlights incidental soil ingestion as an important exposure pathway under the modeled conditions, particularly for children. The lower THI values for adults (Table 4) are consistent with the exposure assumptions used in the model, including lower soil ingestion rates and higher body weight, which result in lower estimated contaminant intake per unit body mass.

Overall, the findings indicate that children represent the more sensitive receptor group under the modeled exposure scenarios. Although individual metals did not exceed the HQ screening threshold, cumulative exposure resulted in THI values above 1.0 at three mining sites. These findings highlight the importance of considering multiple exposure pathways and cumulative contaminant burdens when evaluating potential human-health risks associated with metal-contaminated soils in mining environments.

Carcinogenic risk assessment (CR and TCR)

Children exhibited substantially higher TCR values than adults, with risks approximately 7–8 times higher across the investigated sites (Table 5 and Table S21). This difference is consistent with the exposure assumptions used in the risk model, including children's higher soil ingestion rates and lower body weight. However, these estimates should be interpreted as modeled potential risks rather than predictions of actual cancer incidence, because the calculated values depend on exposure parameters, toxicity values, and assumptions incorporated into the risk-assessment model. The exceedance at SGC indicates that background soil metal concentrations may contribute to the modeled carcinogenic risk; however, the relative contribution of natural versus mining-related sources cannot be established from the CR results alone. Although As, Cd, and Pb contributed less to the calculated CR, their toxicological significance warrants continued consideration because of their established adverse health effects. This pattern indicates that reducing direct soil ingestion could substantially reduce the modeled exposure burden, particularly among children.

Overall, the carcinogenic risk assessment identifies Ni and Cr as the principal contributors to the modeled cancer risk, particularly among children, while cumulative exposure resulted in TCR values above the 1.0×10^{-4} benchmark at all mining sites for children and at SG1–SG3 for adults. These findings highlight the importance of

reducing direct soil exposure and maintaining monitoring and management measures in mining-affected areas. Future studies incorporating metal speciation, bioavailability, site-specific exposure measurements, and biomonitoring would provide a more comprehensive assessment of potential health risks.

The elevated risk estimated for children is particularly relevant to the Osole study setting because mining activities occur in proximity to cultivated land, river corridors, and local settlements. The study area includes permanent and seasonal settlements near mining and riverine environments, where contaminated soil and mine-derived dust may be encountered during routine outdoor activities. Children living in or visiting these environments may therefore have opportunities for direct contact with surface soils and incidental soil ingestion during play and other outdoor activities. Although child-specific behavioral observations were not collected in this study, the combination of residential proximity to mining-affected areas and the age-dependent exposure parameters used in the risk model provides a plausible basis for considering children a vulnerable receptor group.

Limitations

This study was based on a single dry-season sampling campaign (February 2025); therefore, the findings primarily represent contamination conditions during the dry period. Seasonal variations in heavy metal transport, mobility, distribution, and exposure potential could not be fully evaluated. Future studies incorporating multi-season sampling are recommended to better characterize temporal dynamics in mining-affected soils.

A limitation of the present study is the use of air-drying before chemical analysis. Although samples were stored and transported under conditions intended to minimize Hg volatilization, air-drying at room temperature may cause partial Hg loss. Because paired wet- and air-dried samples were not analyzed, the magnitude of any Hg loss cannot be quantified from the present dataset. Consequently, the reported Hg concentrations and Hg-related ecological-risk estimates should be interpreted with this analytical uncertainty in mind.

Furthermore, this study quantified total heavy metal concentrations, whereas the bioavailable fractions controlling mobility and plant uptake were not determined. Future investigations incorporating sequential extraction, bioavailability assessments (e.g., DTPA/EDTA extraction), metal speciation, and soil–plant transfer analyses would provide deeper insight into heavy metal behavior and exposure pathways. Nevertheless, this study establishes an important baseline dataset for understanding heavy metal contamination, ecological risks, and potential human-health implications in the Osole gold-mining area.

Conclusion

This study provides the first integrated assessment of Heavy metal contamination, ecological risks, and human-health implications in soils surrounding the Osole artisanal and small-scale gold mining area, Sidama Regional State, Ethiopia. The results revealed substantial multi-element contamination, with Cd and Hg identified as the dominant contributors to contamination severity and ecological risk. The markedly lower heavy metal concentrations at the reference site compared with mining-influenced locations, together with multivariate statistical relationships, indicate that mining activities are a plausible important contributor, consistent with the observed spatial patterns and site characteristics, although contributions from natural geochemical sources may also influence elemental distribution.

Ecological risk assessment demonstrated high to very high potential risks associated with heavy metal accumulation, particularly due to Cd and Hg enrichment. While individual non-carcinogenic risks remained below acceptable thresholds, cumulative exposure exceeded screening levels for children, emphasizing the importance of evaluating combined contaminant effects. Carcinogenic risk assessment identified Ni and Cr as major contributors, with children representing the most vulnerable receptor group due to higher exposure rates relative to body weight.

The findings establish an important baseline dataset for understanding heavy metal distribution, contamination patterns, and associated risks in an understudied Ethiopian ASGM landscape. The results highlight the need for integrated environmental monitoring, improved mine-waste management, and targeted pollution mitigation strategies to protect agricultural soils and exposed communities. Future studies incorporating seasonal variability, chemical speciation, bioavailability, and soil–crop transfer processes are recommended to further elucidate heavy metal mobility and long-term exposure pathways. Overall, this study provides scientific evidence to support sustainable management of mining-impacted ecosystems in Ethiopia and other emerging ASGM regions.

Acknowledgements

We would like to thank the Sidama Region Environmental and Climate Change Authority for facilitating field sample collection. We also would like to thank the Hawassa University Vice President for Research and Technology Transfer, Research Programs Directorate, for financial support. Our heartfelt appreciation goes to Horticoop. Laboratory PLC, Bishoftu, Ethiopia, for chemical analysis.

Authors' Contribution

Conceptualization: Samuel Bekele, Tesfahun Tesema
Data Curation: Samuel Bekele, Muluken Andemo
Formal Analysis: Samuel Bekele, Teferi Shanka, Tesfahun Tesema
Funding Acquisition: Teferi Shanka
Investigation: Tesfahun Tesema
Methodology: Samuel Bekele, Tesfahun Tesema
Project Administration: Tesfahun Tesema
Resources: Teferi Shanka
Software: Samuel Bekele
Supervision: Tesfahun Tesema
Validation: Samuel Bekele, Teferi Shanka
Visualization: Samuel Bekele
Writing–Original Draft: Samuel Bekele
Writing–Review & Editing: Teferi Shanka, Muluken Andemo, Tesfahun Tesema

Competing Interests
The authors declare that they have no competing interests.

Ethical Approval
This study did not involve human participants, human biological samples, or experimental animals. Soil samples were collected from publicly accessible mining areas in Sidama, Ethiopia, with permission from the Sidama Region Environmental and Climate Change Authority. The research was conducted in accordance with relevant national environmental regulations and institutional research guidelines. All data were generated and analyzed responsibly, and the authors confirm that there was no fabrication, falsification, or inappropriate data manipulation. Proper citation and acknowledgment of all sources have been ensured.

Funding
This study was financially supported by the Vice President for Research and Technology Transfer, Hawassa University.

Supplementary Files
The supplementary file contains Tables S1 – S21.

References
1. Gelaye Y. Public health and economic burden of heavy metals in Ethiopia: Review. Heliyon 2024;10(19): e39022. doi:10.1016/j.heliyon.2024.e39022
2. Wan Y, Liu J, Zhuang Z, Wang Q, Li H. Heavy Metals in Agricultural Soils: Sources, Influencing Factors, and Remediation Strategies. Toxics 2024;12(1):63. doi:10.3390/toxics12010063
3. Samuel B, Solomon S, Daniel F, Zinabu GM, Riise G. *Heavy metals contamination of soil in the vicinity of Hawassa Industrial Zone, Ethiopia*. J Appl Sci Environ Manage. 2020;24(8):1447–1454. doi:10.4314/jasem.v24i8.21
4. Akoto O, Yakubu S, Ofori LA, Bortey-Sam N, Boadi NO, Horgah J, et al. Multivariate studies and heavy metal pollution in soil from gold mining area. Heliyon 2023;9(1): e12661. doi:10.1016/j.heliyon.2022.e12661
5. Rashid A, Schutte BJ, Ulery A, Deyholos MK, Sanogo S, Lehnhoff EA, et al. Heavy Metal Contamination in Agricultural Soil: Environmental Pollutants Affecting Crop Health. Agronomy. 2023;13(6):1521. doi:10.3390/agronomy13061521
6. Chen Y, Liu G, Zhou C, Zhou H, Wei Y, Liu Y. The influence of gold mining wastes on the migration-transformation behavior and health risks of arsenic in the surrounding soil of mined-area. Frontiers in Earth Science 2023;10-2022. doi:10.3389/feart.2022.1068763
7. Fodoué Y, Ismaila A, Yannah M, Wirmvem MJ, Mana CB. Heavy Metal Contamination and Ecological Risk Assessment in Soils of the Pawara Gold Mining Area, Eastern Cameroon. Earth. 2022;3(3):907–24. doi:10.3390/earth3030053
8. Barde BG, Adeleye AO, Oladeji AA, Duhu YB. Heavy metals pollution and ecological risk assessment around artisanal gold mines in Zamfara, Nigeria. Environ Anal Health Toxicol 2024;39(2): e2024016. doi:10.5620/eaht.2024016
9. Getaneh W, Alemayehu T. Metal contamination of the environment by placer and primary gold mining in the Adola region of southern Ethiopia. Environmental Geology 2006;50(3):339–52. doi:10.1007/s00254-006-0213-5
10. Weleabzgi B, Alemayehu T, Estifanos S. Assessing the Environmental Impact of Artisanal Gold Mining Activities on the Waters and Sediments Around Meli, Northwestern Tigray, Ethiopia. Momona Ethiopian Journal of Science 2022;13(2):281–99. doi:10.4314/mejs.v13i2.6
11. Mengistu GT, Sahilu G, Mulat W, Amare E. Assessment of native plants for their potential to remove trace metals around Legadembi tailings dam, Southern Ethiopia. Environ Sci Pollut Res Int 2023;30(19):55615–24. doi:10.1007/s11356-023-26349-y
12. Yimer G. Level of Heavy Metals and Potential Ecological Risks in Irrigated Horticultural Farms in the Vicinity of Lake Ziway, Central Ethiopian Rift Valley Region. J Toxicol 2024;2024:4724097. doi:10.1155/2024/4724097
13. United States Environmental Protection Agency (USEPA), 2002. *Soil Sampling Guidance: Planning, Sampling, and Analysis*. Washington, DC: Office of Emergency and Remedial Response; Report No.: EPA 540-R-01-003
14. Buckley DE, Cranston RE. Atomic absorption analyses of 18 elements from a single decomposition of aluminosilicate. Chemical Geology 1971;7(4):273–84. doi:10.1016/0009-2541(71)90012-X
15. Berrow ML, Mitchell RL. Location of trace elements in soil profiles: total and extractable contents of individual horizons. Transactions of the Royal Society of Edinburgh: Earth Sciences 1980;71(2):103–21. doi:10.1017/S0263593300013547
16. Yüksel B, Kaya S, Kaya-Akyüzlü D, Kayaalti Z, Söylemezoglu T. *Validation and optimization of a cold-vapor AAS method for mercury in maternal blood, cord blood and placenta*. At. Spectrosc. 2017;38(4):112–116. doi:10.46770/AS.2017.04.006
17. Hoogsteen MJJ, Lantinga EA, Bakker EJ, Groot JCJ, Tittonell PA. Estimating soil organic carbon through loss on ignition: effects of ignition conditions and structural water loss. European Journal of Soil Science 2015;66(2):320–8. doi:10.1111/ejss.12224
18. Loring DH, Rantala RTT. Manual for the geochemical analyses of marine sediments and suspended particulate matter. Earth-Science Reviews 1992;32(4):235–83. doi:10.1016/0012-8252(92)90001-A
19. Miller RO, Kissel DE. Comparison of Soil pH Methods on Soils of North America. Soil Science Society of America Journal 2010;74(1):310–6. doi:10.2136/sssaj2008.0047
20. Andrés NB, Ana VS, Leonardo P, Deborah T, Daniel B, Raquel M, et al. Soil texture analyses using a hydrometer: Modification of the Bouyoucos method. Cienc Investig Agrar. 2014;41(2):263–271. doi:10.4067/S0718-16202014000200013
21. Hakanson L. An ecological risk index for aquatic pollution control.a sedimentological approach. Water Research 1980;14(8):975–1001. doi:https:// doi.org/10.1016/0043-1354(80)90143-8
22. Nwankwo RC, Tongu SM, Eneji IS, Nnamonu LA, Wuana RA, Sha'Ato R. Assessment of potential ecological risk of heavy metals in soils from waste dumpsites in military formations in makurdi, Nigeria. J Environ Prot. 2019;10(04):514–31. doi:10.4236/jep.2019.104030
23. Fazekašová D, Fazekaš J. Soil Quality and Heavy Metal Pollution Assessment of Iron Ore Mines in Nizna Slana (Slovakia). Sustainability [Internet]. 2020; 12(6):2549. doi:10.3390/su12062549
24. Kabata-Pendias A. 2001. *Trace Elements in Soils and Plants*, 3rd ed. Boca Raton (FL): CRC Press
25. Alloway BJ. 2013. *Heavy Metals in Soils: Trace Metals and Metalloids in Soils and Their Bioavailability*, 3rd ed. Dordrecht (NL): Springer
26. Xu X, Lu X, Han X, Zhao N. Ecological and health risk assessment of metal in resuspended particles of urban street dust from an industrial city in China. Current Science 2015;108(1):72–9. doi:10.18520/cs/v108/i1/72-79
27. Tomlinson DL, Wilson JG, Harris CR, Jeffrey DW. Problems in the assessment of heavy-metal levels in estuaries and the formation of a pollution index. Helgoländer Meeresuntersuchungen 1980;33(1):566–75. doi:10.1007/BF02414780
28. United States Environmental Protection Agency (USEPA), 2025. *Conducting a Human Health Risk Assessment*. Washington (DC)
29. United States Environmental Protection Agency (USEPA), 1989. *Exposure Factors Handbook*. Office of Health and Environmental Assessment, Washington, DC
30. International Agency for Research on Cancer (IARC), 1980. *Some Metals and Metallic Compounds*. Geneva: World Health

Organization
31. Yüksel B, Kayaalti Z, Kaya-Akyüzlü D, Tekin D, Söylemezoglu T. *Lead levels in maternal blood and their influence on newborns*. At Spectrosc 2016;37(3):114–119. doi:10.46770/AS.2016.03.005
32. Setu S, Strezov V. Impacts of non-ferrous metal mining on soil heavy metal pollution and risk assessment. Sci Total Environ 2025;969:178962. doi:10.1016/j.scitotenv.2025.178962
33. Lemessa F, Simane B, Seyoum A, Gebresenbet G. Analysis of the concentration of heavy metals in soil, vegetables and water around the bole Lemi industry park, Ethiopia. Heliyon 2022;8(12): e12429. doi:10.1016/j.heliyon.2022.e12429
34. Zakaria Sawadogo Y, Luc Bambara T, Zongo I, Kaboré K, Zougmore F. Pollution and Ecological Risk Assessment of Heavy Metals in the Agricultural Soils Around a Gold Mine in BISSA Village, Burkina-Faso. Journal of Environment Pollution and Human Health 2023;11(3):51–59. doi:10.12691/jephh-11-3-1
35. Berego YS, Sota SS, Ulsido M, Beyene EM. The contents of essential and toxic metals in coffee beans and soil in Dale Woreda, Sidama Regional State, Southern Ethiopia. PeerJ 2023;11: e14789. doi:10.7717/peerj.14789
36. Tefera M, Solomon B, Guadie A, Lakew W, Sewachen B, Shumye D. Evaluating the contamination of soil, water and vegetables with heavy metals along with the estimation of transfer factor and human health risk in Gondar city, Ethiopia. Food Safety and Risk 2025;12(1):5. doi:10.1186/s40550-025-00115-z
37. Ustaoğlu F, Yüksel B, Tepe Y, Aydın H, Topaldemir H. Metal pollution assessment in the surface sediments of a river system in Türkiye: Integrating toxicological risk assessment and source identification. Mar Pollut Bull 2024;203:116514. doi:10.1016/j.marpolbul.2024.116514
38. Yüksel B, Ustaoğlu F. *Metals in sediments of lagoon lakes in Türkiye: Toxicological risks and sources*. Process Saf Environ Prot. 2025;193:665–682. doi:10.1016/j.psep.2024.11.085
39. Katsas K, Diamantis DV, Linos A, Psaltopoulou T, Triantafyllou K. The Impact of Exposure to Hexavalent Chromium on the Incidence and Mortality of Oral and Gastrointestinal Cancers and Benign Diseases: A Systematic Review of Observational Studies, Reviews and Meta-Analyses. Environments 2024;11(1):11. doi:10.3390/environments11010011